Deformation of Nuclei Close to the Two-Neutron Drip Line in Mg Region

J. Terasaki, H. Flocard
Division de Physique Théorique[*], Institut de Physique Nucléaire,
F-91406 Orsay Cedex, France

P.-H. Heenen[†]
Service de Physique Nucléaire Théorique,
U.L.B.-C.P.229, B-1050 Brussels, Belgium

P. Bonche
SPhT [‡]-CEA Saclay,F- 91191 Gif sur Yvette Cedex, France

February 5, 2008

Abstract

We present Hartree-Fock-Bogoliubov (HFB) calculations of the ground states of even Mg isotopes. A Skyrme force is used in the mean field channel and a density-dependent zero-range force in the pairing channel. ^{40}Mg and ^{20}Mg are predicted to be at the two-neutron and two proton drip-lines respectively. A detailed study of the quadrupole deformation properties of all the isotopes shows that the ground states of ^{36,38,40}Mg are strongly deformed with significantly different deformations for the neutrons and protons. Our study supports the disappearance of the $N = 28$ shell gap in the Mg and Si isotopes.

[*]Unité de recherches des Universités Paris XI et Paris VI associée au CNRS.
[†]Directeur de Recherches FNRS.
[‡]Laboratoire de la DSM

PACS numbers: 21.10.Dr, 21.10.Pc, 21.60.Jz, 27-30+t, 2740+z

Keywords: Nuclei far from stability; Hartree-Fock Bogoliubov method for deformed nuclei; S_{2n} iand quadrupole moments for Mg isotopes.

1 Introduction

The existence of deformed drip-line nuclei has been recently questionned [1] on the basis of a detailed analysis of the available data. Tanihata et al. have argued that with few exceptions, the last bound isotopes of a chain could be related to a sub-shell closure in a spherical shell model. The number of cases supporting their analysis is however limited since the neutron drip line is known only up to Z=9. A justification relying on results of fully microscopic calculations is not easy to obtain. For evident reasons of simplicity, most studies of drip-line nuclei have been restricted to spherical shapes [2, 3, 4, 5, 6]. ¿From their outcomes, it has been suggested that the single particle gaps associated with magic numbers significantly decrease near the drip lines [2]. Recently, two recent studies of deformation in the Mg[7] and Si-Ca[8] regions in which pairing correlations were described within the constant gap BCS approximation have found sizable deformations for some drip line nuclei. However, no final conclusions can be drawn from these studies since the BCS approximation is known to break down when bound and unbound single-particle states interact via pairing correlations[9].

In a recent publication[10], we have presented a method based on the solution of the Hartree-Fock-Bogoliubov (HFB) equations on a 3-dimensional cartesian mesh. It describes consistently both the pairing correlations and the asymptotic behaviour of the wave functions of weakly bound systems. In this calculation, the effective interaction is considered separately in two different channels: a Skyrme force to describe the mean-field (particle-hole channel) and a density-dependent zero-range force for the pairing correlations (particle-particle channel). Tests of the method on the even Ni isotopes have shown that it accounts correctly for the interactions between bound and continuum single-particle states. Since all the Ni isotopes are spherical, the analysis of the results were easier because of the several degeneracies of single particle and quasi-particle (qp) energies. On the other hand, the potential of investigation of the method is broader than shown by the application

presented in ref.[10]. Indeed, it can as well handle deformed nuclei since all single particle states are calculated within a three-dimensional geometry and allows the description of triaxilly deformed nuclei.

This work is mostly devoted to a study of Mg isotopes. This isotopic chain has been selected because large deformations have been predicted for the heaviest isotopes on the basis of the BCS approximation. Also, together with neighboring isotopic chains, these nuclei have been extensively studied experimentally. Many experimental works have looked for deformation effects at $N = 20$ in the $A = 30$ mass region. Results on isotope shifts of Na isotopes[11, 12] are consistent with an appearance of deformations at $N = 20$ although not yet fully conclusive because the measure of the quadrupole moment of ^{31}Na is still out of reach experimentally. More convincing evidence comes from measurements of masses in ^{31,32}Mg [13], $^{30-32}$Na and $^{31-33}$Mg[14], although is not exempt of ambiguities[15]. However, the flattening of the $S_{2\mathrm{n}}$ curve in Mg isotopes around $N = 20$ appears now to be well established [16]. Systematics of the energies of the first 2^+ states [17] may also be interpreted as a sign of deformation in ^{32}Mg. Finally, a large $B(E2)$ value[18] has recently been measured for the transition between the first 2^+ state and the ground state in ^{32}Mg. Most experimental data point towards the existence of a spherical shell closure at $N = 20$ for the heavier elements: ^{33}Al [19] and $^{33-35}$Si[20, 21, 22]. On the other hand, the vicinity of the one-proton drip line has been explored by Langevin et al. [23] by the observation ^{23}Si, ^{27}S, ^{31}Ar and ^{35}Ca. Recently Suzuki et al. [24] have deduced matter rms radii for a series of Na and Mg isotopes from interaction cross sections.

Several shell-model calculations [25, 26, 27, 28, 29] have been performed for Mg isotopes. They concluded that the inclusion of the f shell is crucial for a correct reproduction of the properties of ^{32}Mg. These studies also support the occurence of prolate quadrupole deformation in ^{32}Mg. Until very recently[30], systematic mean-field calculations in Na and Mg isotopes have not been numerous. The present work contains a drip-line-to-drip-line investigation of the deformation properties of the even Mg isotopes. In addition, at the neutron drip line, we have also studied the neighbouring even Z elements (Ne and Si).

2 Strength of the pairing interaction

In our method, distinct parametrizations for the interaction are chosen for the mean-field and the pairing channels. For the particle-hole channel, a Skyrme force is used. We have studied two well established parameter sets. The first one is SIII [31], which has been extensively and often successfully used to study deformation properties. The second one, Sly4 [32] is more recent. It has been constructed with a special attention paid to the properties of nuclear matter and neutron matter. It is therefore expected to provide a more realistic isospin dependence than previous forces. With such a choice of two parametrizations of the effective force which are known to work equally well in the region of stable nuclei should provide a measure of the uncertainity of microscopic effective theory at large T_z.

For the pairing channel, a density-dependent zero-range force is used:

$$V_{\mathrm{P}}(\mathbf{r}_1,\mathbf{r}_2) = V_0(1-P_\sigma)(1-\frac{\rho(\mathbf{r}_1)}{\rho_{\mathrm{c}}})\,\delta(\mathbf{r}_1-\mathbf{r}_2) \quad , \tag{1}$$

where P_σ is the spin exchange operator and $\rho(\mathbf{r})$ the total nuclear density. V_0 is the strength of the force, chosen to be the same for neutrons and protons, and ρ_{c} is a constant which determines the density dependence. In this work we take ρ_{c} equal to $0.16\mathrm{fm}^{-3}$. With such a value close to the nuclear saturation density, the pairing force is strongly attractive at the nuclear surface. This property has been discussed in [4] (see also ref[33]). A smooth cut-off of the pairing interaction at an energy of 5 MeV above the fermi level has been introduced following the procedure explained in ref[34].

In ref. [10], we have shown that our numerical method provides reliable results for the properties of drip line nuclei when two numerial conditions are satisfied. Firstly, the dimension of the box in which the HF equations are solved must be large enough to describe correctly the tail of the wave functions. Secondly, since the imaginary time method used to solve the mean-field equations can only be applied to a limited number of orbitals, the number of these orbitals must be large enough to ensure a correct description of the continuum wave functions ; especially those associated with the low-lying resonance states. In the present application to Mg isotopes, we have used values for the box size (15 fm) and for the number of single-particle wave functions (70 for neutrons and 35 for protons) that have been shown

to be sufficient in the calculation of Ni isotopes. Since this study is devoted to much lighter nuclei, we are confident that these values are adequate. We have also checked this point with tests on a selection of nuclei, which have confirmed the conclusions of the previous study.

The Mg isotopes are not an optimal region of the nuclear chart for an adjustment of the pairing strength V_0. Indeed, due to the weakness of pairing correlations in light nuclei, the determination of experimental qp energies from binding energies is not very accurate. Moreover, the variation of these binding energies is affected by the strong dependence of the shape of Mg isotopes on the neutron number, which must be taken into account in the process determining the qp energies. Previous studies of superdeformation in both the A=150 and 190 mass regions have shown that the value $V_0 = 1000\mathrm{MeVfm}^3$ for SIII and SLy4 gives results of good quality. We have therefore investigated whether one could use these values for the Mg isotopes. To this end, we have compared the experimental and theoretical values obtained for the two-neutron separation energies $S_{2\mathrm{n}}(N,Z)$, calculated from the difference between the HFB ground state energies of neighbouring even nuclei. The quantity $-2\lambda_n$, where λ_n is the HFB chemical potential, provides another approximation of $S_{2\mathrm{n}}(N,Z)$. In order to investigate the sensitivity of results to V_0, we have repeated some calculations with the value V_0=700MeVfm^3. Results are plotted on Fig. 1 together with the experimental data. The $S_{2\mathrm{n}}$ values are almost insensitive to V_0. They are also rather similar for both Skyrme parametrizations. The general features of the experimental data are satisfactorily reproduced. Experimentally, the shell effect at N=20 disappears in ^{32}Mg in agreement with the large scale shell model calculations of ref [29]. In this respect, the results obtained with SIII are more consistent with the experimental data than those obtained with SLy4, although in both cases the shell effect is weak. The problems associated with the description of ^{32}Mg will be discussed in a forthcoming publication.

Since the strength $V_0 = 1000\mathrm{MeVfm}^3$ gives a reasonnable agreement with the experimental data for the $S_{2\mathrm{n}}$ values, we have decided to use it for both SIII and SLy4. We have also checked that it leads to qp energies in ^{24}Mg close to the experimental ones. More importantly, the fact that the same value can be used for light nuclei and for heavy superdeformed ones is a first indication that a unique parametrization of a density-dependent zero-

range pairing interaction may be valid in the whole nuclear chart. With the adopted strength, pairing correlations vanish for protons in $^{36-40}$Mg and for neutrons in ^{20}Mg and ^{26}Mg.

On Fig. 2, we compare the experimental data for $S_{2\mathrm{n}}$ as a function of A [16] to the prediction of different models. In our calculations the two-neutron drip line is located between ^{40}Mg and ^{42}Mg for both SIII and SLy4. The lightest Mg isotope predicted to be bound against two proton decay is ^{20}Mg. Its two-proton separation energy calculated with SIII is equal to 3.31 MeV; a number that is to be compared with the experimental value 2.33 MeV. Other theoretical approaches designed to reproduce nuclear masses lead to a better agreement with data than our calculation. However, outside the experimentally known region, their predictions for $S_{2\mathrm{n}}$ show irregularities the interpretation of which is difficult. Nevertheless, the trends obtained with the relativistic mean field (RMF) theory [7] and the finite-range droplet model (FRDM) [35], are similar except for ^{20,22}Mg and for a slight increase of $S_{2\mathrm{n}}$ from ^{38}Mg to ^{40}Mg in the FRDM. Thus it seems that the location of the two-neutron drip line does not depend very much on the theoretical approach, at least for the three types of methods we have just quoted. Hereafter we shall discuss the results obtained with SIII unless otherwise specified.

3 Deformation properties of the Mg isotopes

Fig. 3 shows the variation of the energy of the stable Mg isotopes as a function of their axial quadrupole moment. As expected, the energy curve of ^{20}Mg displays the well defined spherical minimum that one expects for the magic neutron number N=8. In light isotopes, there is a competition between oblate and prolate deformations. All deformed isotopes turn out prolate with the exception of ^{26}Mg. In the heavier isotopes, a deformed shell effect appears. It is already visible on the deformation energy curve of ^{32}Mg which displays an inflection point at Q=1.5b. We find well defined prolate minima from ^{36}Mg to the drip line nucleus ^{40}Mg. In these three cases, a very shallow oblate minimum appears at an excitation energy of 1.0 MeV. We therefore find that the neutron shell effect at $N = 28$ is suppressed at the drip line. ¿From our calculations, it turns out that the onset of deformations at N=24 only generates a drop of about 1MeV in the curve of the evolution of $S_{2\mathrm{n}}$

versus the neutron number.

Since ^{40}Mg is bound by less than 2.0 MeV, we have checked if the large quadrupole moment of the ground state was not caused by a neutron halo which our calculation may not describe properly. To test the numerical quality of our results concerning the space distribution of outer neutrons, we have verified whether the number of neutrons outside a sphere of large radius (r >15 fm)

$$N_{\rm out} = \int_{r \geq 15 {\rm fm}} \rho_{\rm n}(\mathbf{r})\ d^3\mathbf{r}\ , \tag{2}$$

was stable against the box size R ($\rho_{\rm n}(\mathbf{r})$ is the neutron density). We find $N_{\rm out}$ to be 0.430×10^{-2} and 0.683×10^{-2} for box sizes R = 16 and 18 fm, respectively. These small and almost constant values indicate the absence of a halo in ^{40}Mg. In order to determine which part of the nuclear density is responsible for the calculated deformation, we have introduced quantities $\beta_\tau(r_{\rm in})$ ($\tau = n, p$) depending on a cutoff variable $r_{\rm c}$:

$$\beta_\tau(r_{\rm c}) = (\pi/5)^{1/2} \frac{\overline{Q_\tau}(r_{\rm c})}{\overline{r_\tau^2}(r_{\rm c})} \quad . \tag{3}$$

The quantities $\overline{r_\tau^2}(r_{\rm c})$ and $\overline{Q_\tau}(r_{\rm c})$ defined by

$$\overline{r_\tau^2}(r_{\rm c}) = \int_{r \leq r_{\rm c}} r^2 \rho_\tau(\mathbf{r})\ d^3\mathbf{r}\ , \quad \overline{Q_\tau}(r_{\rm c}) = \int_{r \leq r_{\rm c}} Q(\mathbf{r}) \rho_\tau(\mathbf{r})\ d^3\mathbf{r}\ , \tag{4}$$

are respectively the square radius and the quadrupole moment values of the fraction of the nuclear density inside the sphere of radius $r_{\rm c}$. ¿From the results shown on Fig. 4 for ^{40}Mg one sees that the asymptotic values of the deformations β_τ are reached when $r_{\rm in}$ is equal to 6.0 fm. This value is precisely equal to the 5/3rd of the root-mean-square radius of the nucleus (3.6 fm) and corresponds therefore to the sharp edge liquid drop value of the outer radius. This demonstrates that the neutron and proton deformation, β_n and β_p, reflect a property of the distributions of core nucleons.

The neutron and proton parameters β_n and β_p and the total quadrupole moments are plotted in Fig. 5 for all the Mg isotopes. Values of β and of the quadrupole moments of secondary minima are also indicated. Due to the conjunction of the $N = Z$ =12 deformed shell effects, the nucleus ^{24}Mg is the most deformed of the isotope chain. In our calculation, the spherical

shell closure at N=20 is strong enough to compensate the effect of the proton deformed shell closure. On the other hand, we have mentioned above that the deformation energy curve of ^{32}Mg [see Fig. 3] displays an inflexion point at a prolate deformation. This is the first indication of the deformed shell effect which determines the shape of the deformation energy curves of the heavier isotopes. The values of β_n and β_p for this inflexion point are reported on Fig. 5. As the $f_{7/2}$ shell begins to be filled, the magnitude of the spherical neutron shell effect decreases and allows the proton deformed shell effect to take over in $^{36-40}$Mg. In these nuclei, one recovers a proton deformation similar to that found for ^{24}Mg. The experimental evidence based on the existence of a low energy 2^+ state with a large B(E2) value [18] in ^{32}Mg implies that our calculation overestimates the magnitude of the spherical N=20 shell effect in this nucleus. With two other Skyrme parametrizations, Sly4 and SkP [9], we also find that the deformation energy curve for ^{32}Mg presents a spherical minimum. To our knowledge, this is also the case for all mean-field calculations whether they include a treatment of pairing correlations[27] or not. Apart from ^{32}Mg, data on deformation are few with generally large error bars. Still they are consistent with values of β larger than those we have calculated. We believe that this systematic effect reflects the approximate character of the the prescription (3) that we use to define β_p. Indeed, it is implicitly based on a sharp edge liquid drop picture which neglegts surface effects which could be of importance in such light nuclei. Keeping this restriction in mind, we note that for light isotopes, the values of β_n and β_p are similar, while they differ for the last three heavy isotopes. With mean-field effective forces, differing deformations are more easy to obtain when there is a large excess of neutrons over protons. Indeed, for nuclei close to the stability line, the large overlap between the neutron and proton densities and the strongly attractive neutron-proton interaction have a tendancy to suppress the differences of deformations. This is indeed what we find for the light magnesiums. In view of our results, it appears worthwhile to experimentally investigate whether heavy Mg isotopes would not be the lightest examples of nuclei with differing neutron and proton deformations.

On Fig.6, one sees that the calculated root-mean-square radii stay within the error bars of the measured data. The onset of deformation in ^{36}Mg causes a slight irregularity in the calculated curves. An irregularity of the

same magnitude does not seem to be present in the experimental data around ^{32}Mg.

The single particle level energies in the canonical Hartree-Fock-Bogoliubov basis are shown on Fig. 7 for ^{40}Mg. Apart from a global shift in energy, a similar diagram is valid for all Mg isotopes. In ^{40}Mg, at the quadrupole moment of the deformed ground state, the neutron fermi level is close to the continuum. The large density of levels at the fermi surface provides an explanation for the smaller neutron deformation (compared to proton). Indeed, because it enhances the effect of pairing correlations, it induces a population of orbitals with a less deformation driving character than the $\pi d_{5/2}$ orbital.

Results qualitatively similar to ours have been obtained in the RMF calculation of Ren et al.[7]. Both ^{20}Mg and ^{32}Mg have been found spherical by these authors and $^{36-40}$Mg very deformed. However, the quadrupole moments of deformed isotopes are significantly larger in the RMF calculation. This may be related to the BCS approximation with a constant gap used by Ren et al.

The $N = 28$ neutron gap does show up as an accident neither in the S_{2n} curve nor in the evolution of the radii. On Fig. 7, one sees that the value of the N=28 single particle gap is about 3 MeV in ^{40}Mg. This is much smaller than the gap that one finds in ^{48}Ca (5MeV) with a calculation using the same effective force[31]. This quenching of the $N = 28$ gap is sufficient to allow the deformed proton gap at $Z = 12$ to win over the spherical shell effect and to lead to a deformed nucleus. Similar results have been obtained in a recent study of Si and S isotopes [8].

Fig. 8 shows the potential energy curve of the nucleus ^{42}Si ($N = 28$). The same figure displays the curves of the two nuclei ^{34}Ne and ^{46}Si which according to our method are on the drip line. The energy curves of these three isotopes display a soft dependence on the quadrupole moment. This suggests that dynamical quadrupole collective effects may play an important rôle. One notes also that, as was the case already for ^{40}Mg, there is no indication of a spherical shell effect at $N = 28$ for ^{42}Si. Similar results have been obtained by Werner et al[8] with the HF+BCS approximation.

4 Conclusion

In this paper, we have reported the first calculation of the deformation properties of drip line nuclei using a Hartree-Fock-Bogoliubov approach in which pairing correlations in the continuum are correctly treated.

Our work shows that deformation effects cannot be neglected in a description of the structure of neutron rich Mg isotopes. In particular, it provides a negative answer to the question raised by Tanihata et al [1] as to whether all drip line nuclei are spherical.

Another conclusion of this work, is that the N=28 spherical shell closure is significantly weakened in light nuclei close to the drip line. As a consequence, we find that the deformation properties of heavy Mg isotopes are more influenced by the proton deformed shell effect at Z=12 than by the neutron spherical shell closure at N=28. Due to pairing correlations, the population of neutron deformation driving orbits favours the occurence of deformation in the last bound Mg isotopes.

Finally, we find that with the prescription that we introduce to define deformations, the large excess of neutrons with respect to the protons leads non zero differences $(\beta_n - \beta_p)$ in the heavy Mg isotopes. A confirmation of this property would be the existence of low lying quadrupole isovector excitation for isotopes close to the drip lines.

Therefore, the several original properties predicted by our calculation give an additional incentive to the pursuit of a more thorough investigation of this section of neutron drip line.

Acknowledgments

This research was supported in part by the Belgian Office for Scientific Policy under Contract ARC 93/98-166.

References

[1] I. Tanihata, D. Hirata and H. Toki, Nucl. Phys. A**583** (1995) 769

[2] J. Dobaczewski, I. Hamamoto, W. Nazarewicz and A. Sheikh, Phys. Rev. Lett. **72** (1994) 981

[3] J. Dobaczewski, W. Nazarewicz and T. R. Werner, Z. Phys. A **354** (1996) 27

[4] J. Dobaczewski, W.Nazarewicz, T. .R. Werner, J. F. Berger, C. R. Chinn and J. Decharge, Phys. Rev C **53** (1996) 2809

[5] D. Hirata, H. Toki, T. Watabe, I. Tanihata and B. V. Carlson, Phys. Rev. C **44** (1991) 1467

[6] R. Smolańczuk and J. Dobaczewski, Phys. Rev. C **48** (1993) R2166

[7] Z. Ren, Z. Y. Zhu, Y. H. Cai and G. Xu, Phys. Lett. B **380** (1996) 241

[8] T.R. Werner, J.A. Sheikh, M. Misu, W. Nazarewicz, J. Rikovska, K. Heeger, A.S. Umar and M.R. Strayer, Nucl. Phys. **A597** (1996) 327

[9] J. Dobaczewski, H. Flocard and J. Treiner, Nucl. Phys. **A422** (1984) 103

[10] J. Terasaki, P.-H. Heenen, H. Flocard and P. Bonche, Nucl. Phys. A **600** (1996) 371

[11] G. Huber et al. Phys. Rev. C **18** (1978) 2342

[12] F. Touchard et al. Phys. Rev. C **25** (1982) 2756

[13] C. Détraz et al. Nucl. Phys. A **394** (1983) 378

[14] A. Gillibert et al. Phys. Lett. B **192** (1987) 39

[15] D. J. Vieira et al. Phys. Rev. Lett. **57** (1986) 3253

[16] G. Audi and A. H. Wapstra, Nucl. Phys. A **565** (1993) 66

[17] C. Détraz, et al. Phys. Rev. C **19** (1979) 164

[18] T. Motobayashi et al., Phys. Lett. B **346** (1995) 9

[19] D. J. Woods et al. Phys. Lett. B **182** (1986) 297

[20] P. J. Woods et al. Z. Phys. A **321** (1985) 119

[21] L. K. Fifield et al. Nucl. Phys. A **440** (1985) 531

[22] R. J. Smith et al. Z. Phys. A **324** (1986) 283

[23] M. Langevin et al. Nucl. Phys. A **455** (1986) 149

[24] T. Suzuki et al. private communication

[25] B. H. Wildenthal and W.Chung, Phys. Rev. C **22** (1980) 2260

[26] A. Watt, R. P. Singhal, M. H. Storm and R. R. Whitehead, J. Phys. G **7** (1981) L145

[27] A. Poves and J. Retamosa, Phys. Lett. B **184** (1987) 311; Nucl. Phys A **571** (1994) 221

[28] E. K. Warburton, J. A. Becker and B. A. Brown, Phys. Rev. C **41** (1990) 1147

[29] N. Fukunishi, T. Otsuka and T. Sebe, Phys. Lett. B **296** (1992) 279

[30] X. Campi, H. Flocard, S. Koonin and A.K. Kerman, Nucl. Phys. A **151** (1975) 193

[31] M. Beiner, H. Flocard, N. Van Giai and P. Quentin, Nucl. Phys. A **238** (1975) 29

[32] E. Chabanat, P. Bonche, P. Haensel and R. Schaeffer, Phys. Script. **T56** (1995) 231, and private communication.

[33] V.E. Starodubsky and M.V. Zverev Phys Lett **B276** (1992) 269

[34] P. Bonche, H. Flocard, P.-H. Heenen, S.J. Krieger and M.S. Weiss, Nucl. Phys. A **443** (1985) 39

[35] P. Möller, J. R. Nix, W. D. Myers and W. J. Swiatecki, Atom. Data and Nucl. Data Tables **59** (1995) 185

[36] D. Schwalm et al., Nucl. Phys. A **192** (1972) 449

[37] E. W. Lees et al., J. Phys. G **2** (1976) 105

Figure Captions

Fig. 1 Calculated and experimental S_{2n} of Mg isotopes for $A = 22-34$. with two Skyrme force parametrizations: (a) SIII and (b) SLy4. In both cases, two strengths of the pairing force are tested: $V_0 = 1000$ and 700 MeV fm^3.

Fig. 2 Calculated and experimental S_{2n} from the proton to the neutron drip lines. Our results are obtained with the SIII parametrization. Results of RMF and FRDM calculations are taken from refs. [7] and [35], respectively.

Fig. 3 Deformation energy curves calculated for the even $^{20-40}$Mg isotopes with SIII as a function of the axial quadrupole moment. The origin of the energy is taken at the minimum of each curve.

Fig. 4 Deformation parameter β for protons and neutrons in ^{40}Mg calculated as a function of the cut-off radius $r_{\rm in}$. See eqs. (3) and (4).

Fig. 5 Deformation parameter β (upper panel) and total quadrupole moments (lower panel) of the Mg isotopes versus A. Ground state values are connected by lines. Isolated symbols correspond to the secondary minima found for some isotopes. Black symbols correspond to absolute or secondary minima, open symbols to shoulder in the deformation energy curves of Fig. 3. The β deduced from the experimental data have been taken from refs. [36] and [37] for ^{24,26}Mg and from [18] for ^{32}Mg.

Fig. 6 Calculated and experimental rms radii versus A. The theoretical values are joined by lines. The black stars are the matter rms radii of ref.[24], and the white stars are the charge rms radii of ref.[37].

Fig. 7 Single-particle energy diagram of ^{40}Mg as a function of the total quadrupole moment. These energies are the diagonal matrix elements of the HF Hamiltonian in the canonical basis. The upper and lower parts are for neutrons and protons respectively.

Fig. 8 Deformation energy curves of ^{34}Ne and ^{42,46}Si as a function of the axial quadrupole moment.

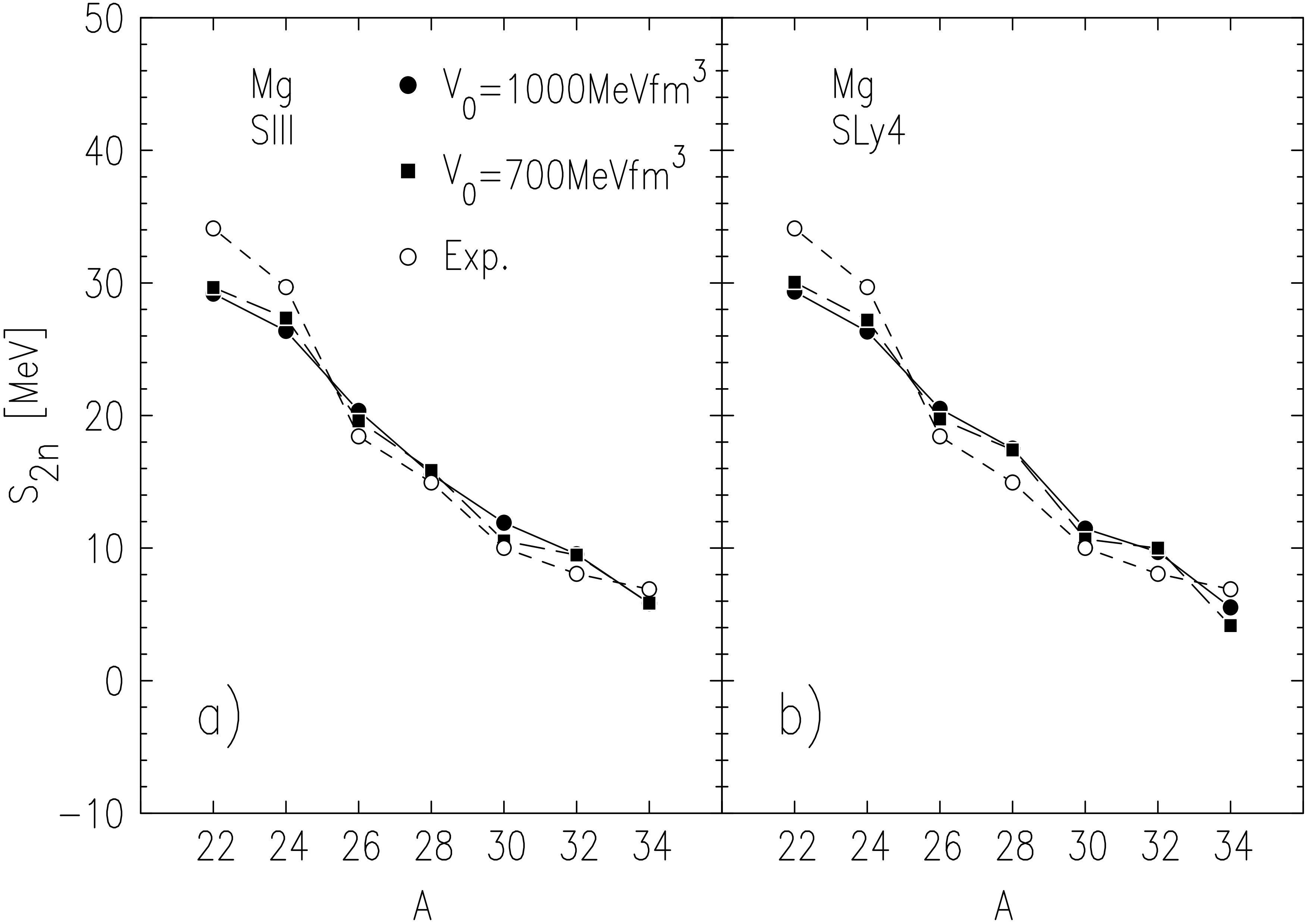

S_{2n} [MeV]
50
40
30
20
10
0
−10
Mg
SIII
V_0=1000MeVfm^3
V_0=700MeVfm^3
Exp.
a)
Mg
SLy4
b)
22 24 26 28 30 32 34
A

Fig.1

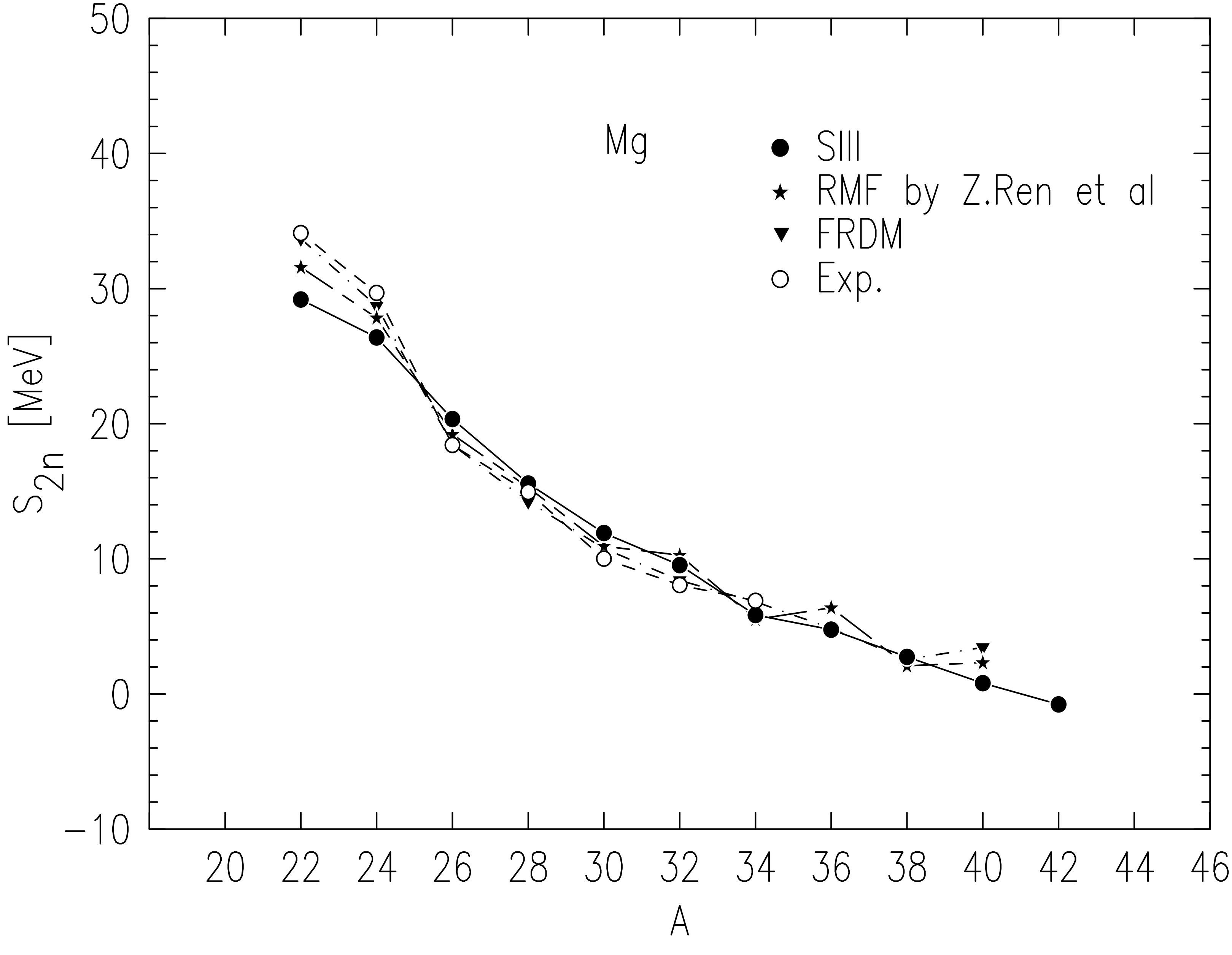
Mg
SIII
RMF by Z.Ren et al
FRDM
Exp.
S2n [MeV]
A
50
40
30
20
10
0
−10
20
22
24
26
28
30
32
34
36
38
40
42
44
46

Fig.2

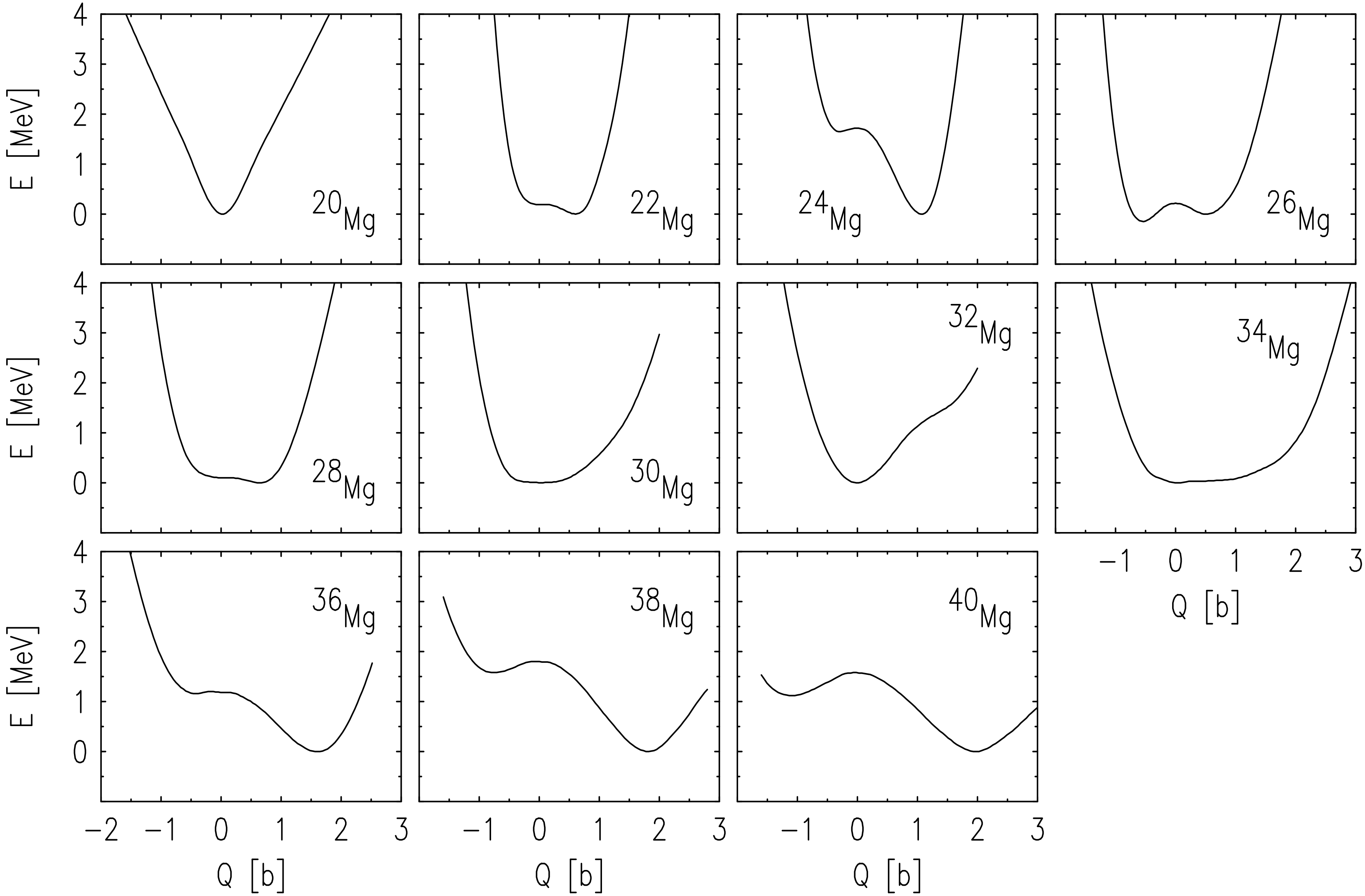
E [MeV]
Q [b]
^{20}Mg
^{22}Mg
^{24}Mg
^{26}Mg
^{28}Mg
^{30}Mg
^{32}Mg
^{34}Mg
^{36}Mg
^{38}Mg
^{40}Mg

Fig.3

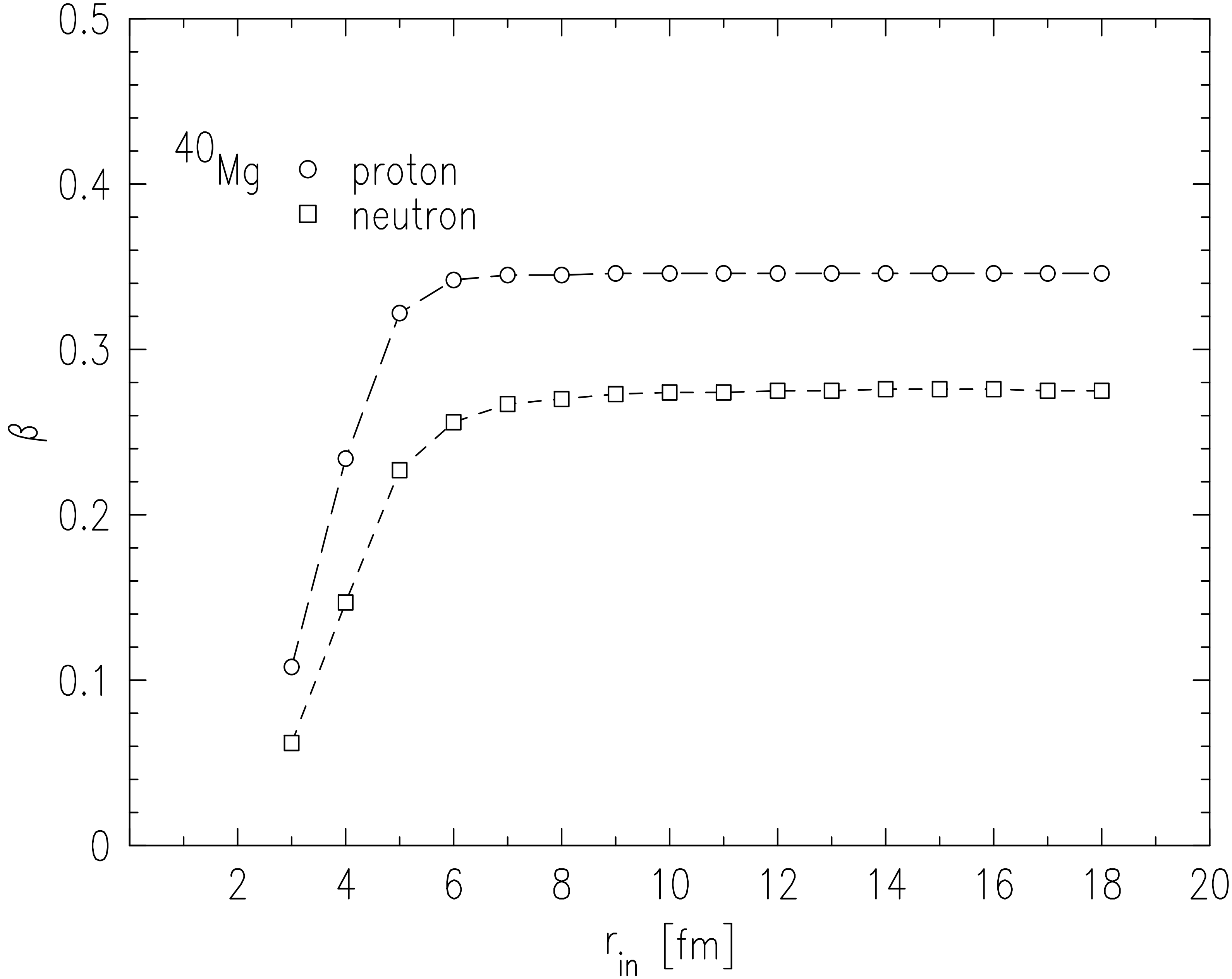

0.5
0.4
0.3
0.2
0.1
0
β
40Mg
proton
neutron
2
4
6
8
10
12
14
16
18
20
r_in [fm]

Fig.4

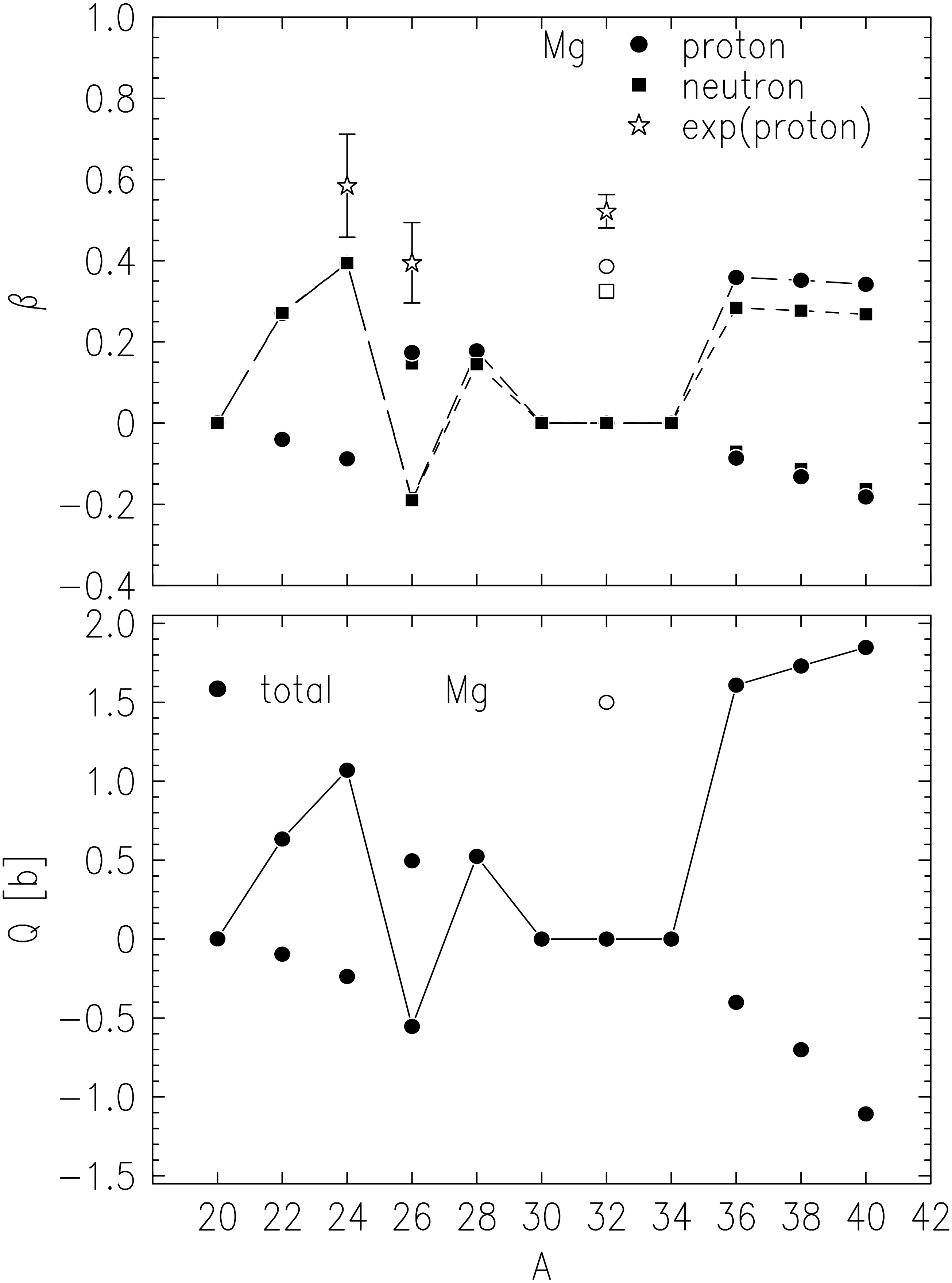

Mg
proton
neutron
exp(proton)
β
total
Mg
Q [b]
A
1.0
0.8
0.6
0.4
0.2
0
−0.2
−0.4
2.0
1.5
1.0
0.5
0
−0.5
−1.0
−1.5
20
22
24
26
28
30
32
34
36
38
40
42

Fig.5

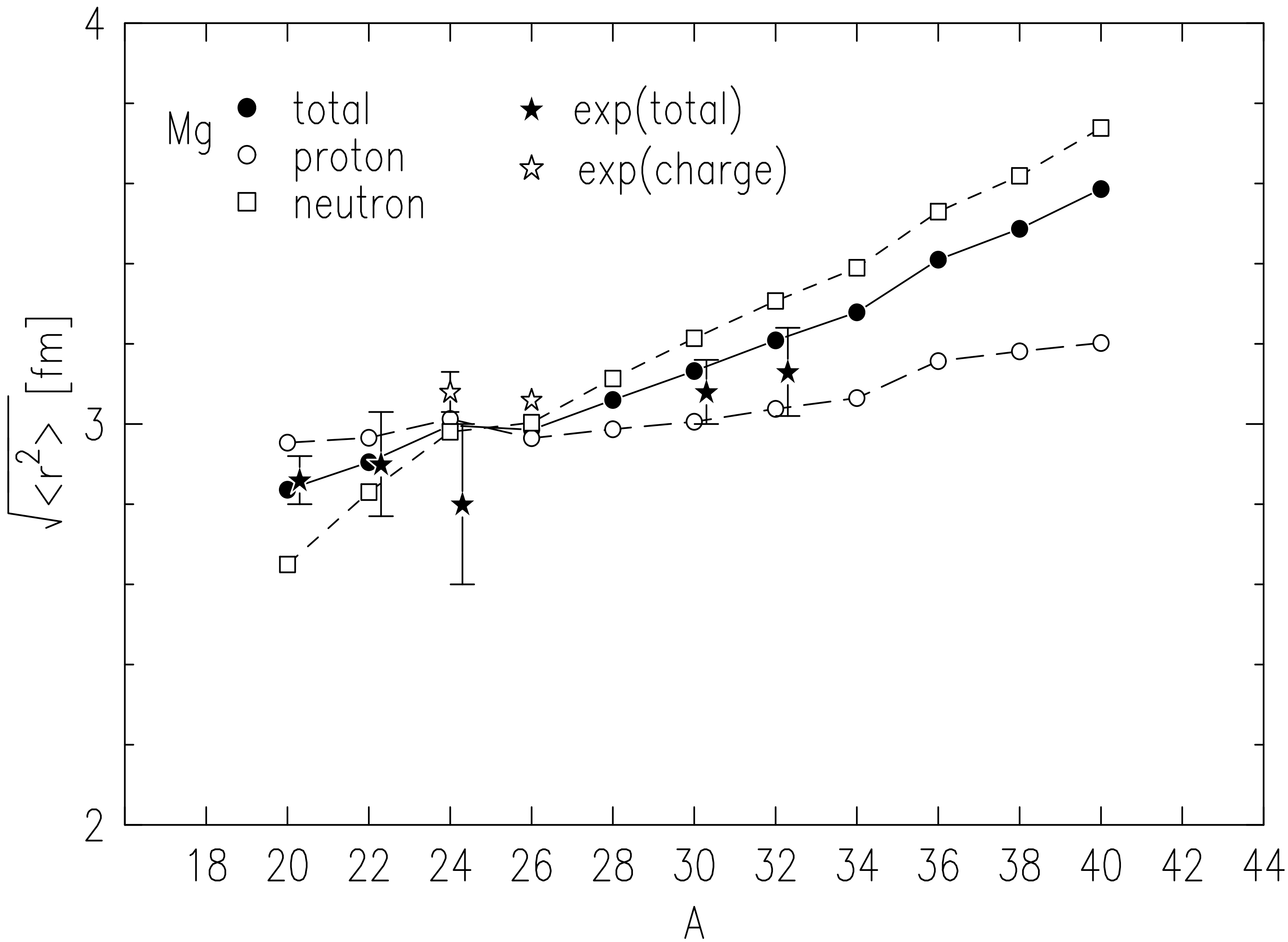

Mg
total
proton
neutron
exp(total)
exp(charge)
$\sqrt{\langle r^2 \rangle}$ [fm]
4
3
2
18
20
22
24
26
28
30
32
34
36
38
40
42
44
A

Fig.6

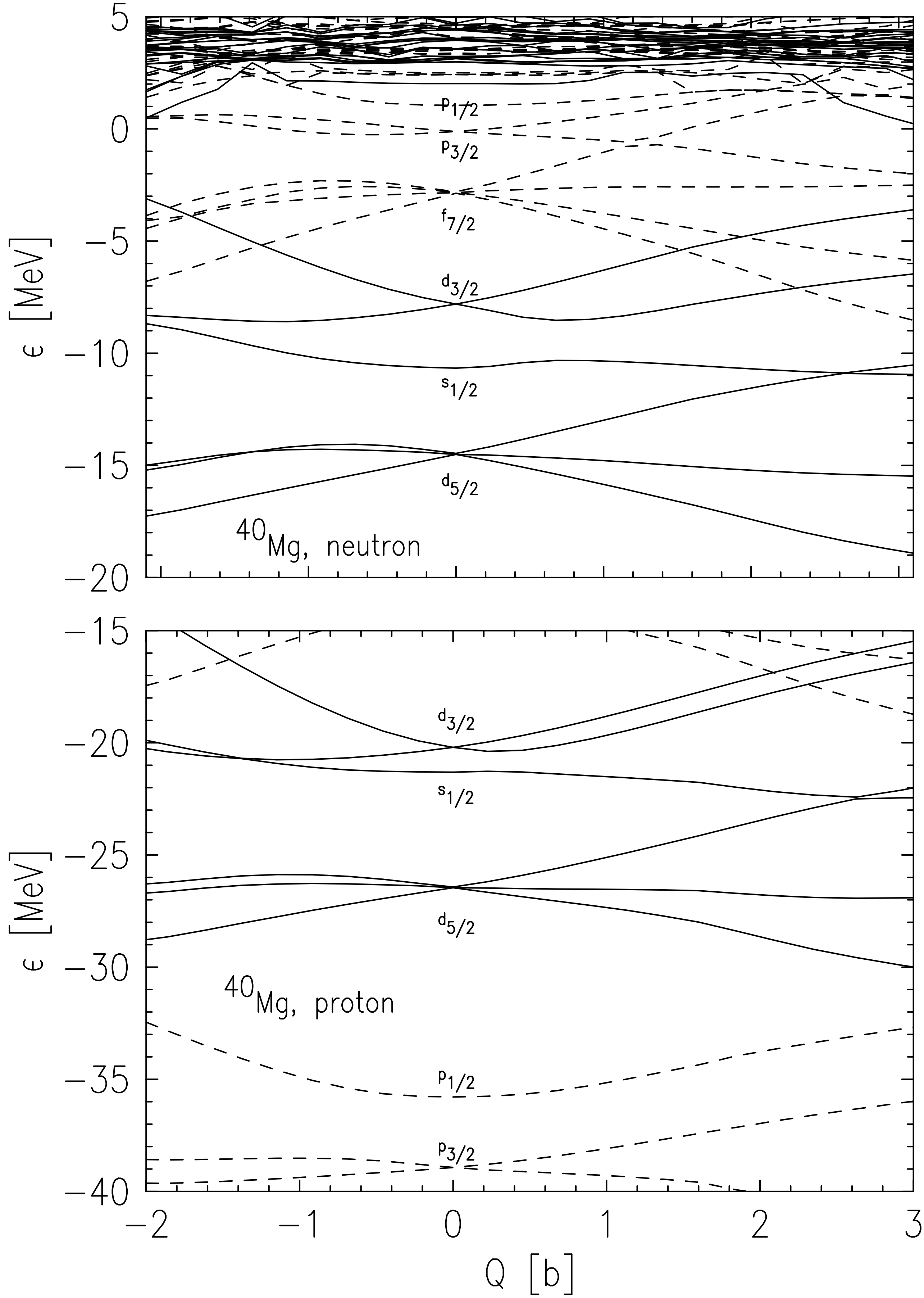

5
0
−5
−10
−15
−20
ε [MeV]
$p_{1/2}$
$p_{3/2}$
$f_{7/2}$
$d_{3/2}$
$s_{1/2}$
$d_{5/2}$
^{40}Mg, neutron
−15
−20
−25
−30
−35
−40
ε [MeV]
$d_{3/2}$
$s_{1/2}$
$d_{5/2}$
^{40}Mg, proton
$p_{1/2}$
$p_{3/2}$
−2
−1
0
1
2
3
Q [b]

Fig.7

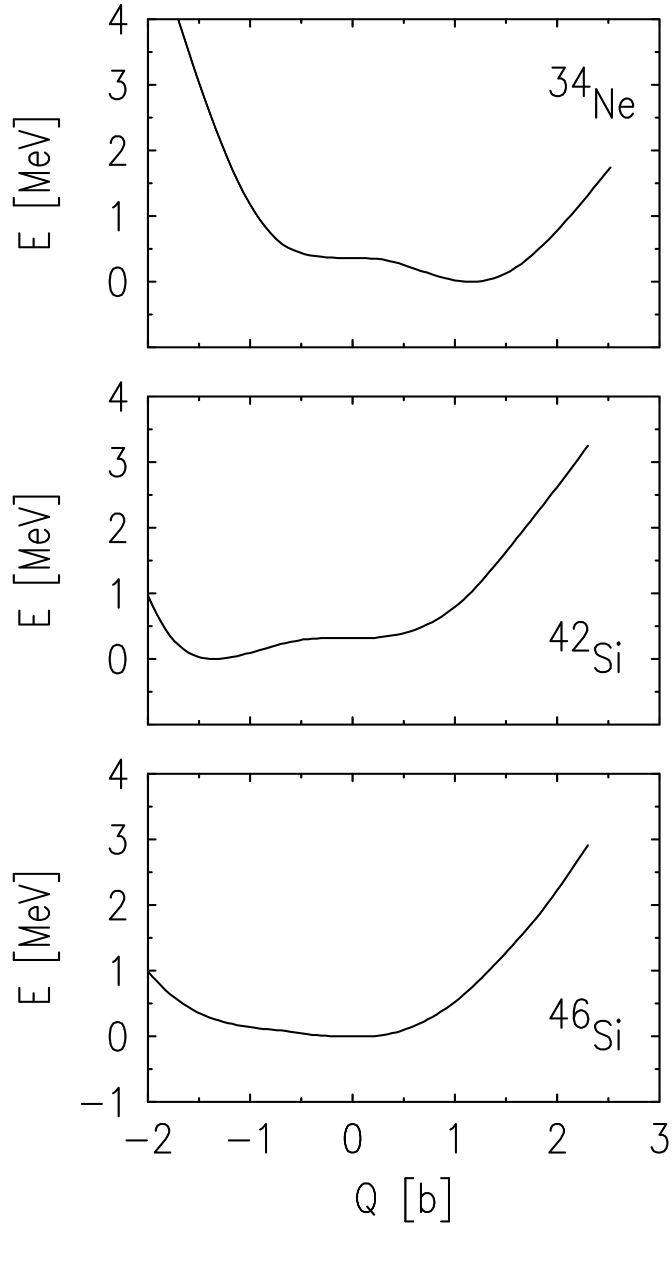

Fig.8